AMERICAN SOCIETY FOR MICROBIOLOGY | mSphere®

Spatiotemporal Distribution of *Pseudomonas aeruginosa* Alkyl Quinolones under Metabolic and Competitive Stress

Tianyuan Cao,[a] Jonathan V. Sweedler,[b,c] Paul W. Bohn,[a,d,e] Joshua D. Shrout[e,f,g,h]

[a]Department of Chemistry and Biochemistry, University of Notre Dame, Notre Dame, Indiana, USA
[b]Department of Chemistry, University of Illinois at Urbana-Champaign, Urbana, Illinois, USA
[c]Beckman Institute for Advanced Science and Technology, University of Illinois at Urbana-Champaign, Urbana, Illinois, USA
[d]Department of Chemical and Biomolecular Engineering, University of Notre Dame, Notre Dame, Indiana, USA
[e]Advanced Diagnostics and Therapeutics, University of Notre Dame, Notre Dame, Indiana, USA
[f]Department of Civil and Environmental Engineering and Earth Sciences, University of Notre Dame, Notre Dame, Indiana, USA
[g]Department of Biological Sciences, University of Notre Dame, Notre Dame, Indiana, USA
[h]Eck Institute for Global Health, University of Notre Dame, Notre Dame, Indiana, USA

ABSTRACT *Pseudomonas aeruginosa* is an opportunistic human pathogen important to diseases such as cystic fibrosis. *P. aeruginosa* has multiple quorum-sensing (QS) systems, one of which utilizes the signaling molecule 2-heptyl-3-hydroxy-4-quinolone (*Pseudomonas* quinolone signal [PQS]). Here, we use hyperspectral Raman imaging to elucidate the spatiotemporal PQS distributions that determine how *P. aeruginosa* regulates surface colonization and its response to both metabolic stress and competition from other bacterial strains. These chemical imaging experiments illustrate the strong link between environmental challenges, such as metabolic stress caused by nutritional limitations or the presence of another bacterial species, and PQS signaling. Metabolic stress elicits a complex response in which limited nutrients induce the bacteria to produce PQS earlier, but the bacteria may also pause PQS production entirely if the nutrient concentration is too low. Separately, coculturing *P. aeruginosa* in the proximity of another bacterial species, or its culture supernatant, results in earlier production of PQS. However, these differences in PQS appearance are not observed for all alkyl quinolones (AQs) measured; the spatiotemporal response of 2-heptyl-4-hydroxyquinoline *N*-oxide (HQNO) is highly uniform for most conditions. These insights on the spatiotemporal distributions of quinolones provide additional perspective on the behavior of *P. aeruginosa* in response to different environmental cues.

IMPORTANCE Alkyl quinolones (AQs), including *Pseudomonas* quinolone signal (PQS), made by the opportunistic pathogen *Pseudomonas aeruginosa* have been associated with both population density and stress. The regulation of AQ production is known to be complex, and the stimuli that modulate AQ responses are not fully clear. Here, we have used hyperspectral Raman chemical imaging to examine the temporal and spatial profiles of AQs exhibited by *P. aeruginosa* under several potentially stressful conditions. We found that metabolic stress, effected by carbon limitation, or competition stress, effected by proximity to other species, resulted in accelerated PQS production. This competition effect did not require cell-to-cell interaction, as evidenced by the fact that the addition of supernatants from either *Escherichia coli* or *Staphylococcus aureus* led to early appearance of PQS. Lastly, the fact that these modulations were observed for PQS but not for all AQs suggests a high level of complexity in AQ regulation that remains to be discerned.

KEYWORDS PQS, HQNO, *Staphylococcus aureus*, polymicrobial, quorum sensing, Raman spectroscopy, principal-component analysis, chemical imaging

Pseudomonas aeruginosa is a ubiquitous Gram-negative bacterium and an opportunistic human pathogen that can be found in soil and freshwater and also in infection environments, such as the lungs of cystic fibrosis patients (1, 2). Like many other bacterial species, P. aeruginosa can coordinate group behaviors, such as surface movement, biofilm formation, and virulence factor production, using several mechanisms. One mechanism of coordination utilizes a communication system known as quorum sensing (QS), whereby individual cells, secrete, release, and sense chemical signal molecules (3, 4), enabling responses to environmental challenges in a cooperative and coordinated way to improve bacterial survival (5–8). P. aeruginosa uses four interconnected QS signaling systems, i.e., the Las, Rhl, PQS (Pseudomonas quinolone signal), and IQS (integrated quorum-sensing) systems (9), which are organized in a multilayered and intertwined hierarchy.

The PQS system uses 2-alkyl-4(1H)-quinolones (AQs) (10) to mediate bacterial behaviors, including iron chelation, cytotoxicity, and other functions associated with virulence (11–13). The regulation of AQ production, not just PQS production, is complex. Synthesis of the AQs first requires activity encoded by the pqsABCD operon to act upon the precursor anthranilic acid (14, 15). Induction of pqsABCD is regulated by the Las quorum-sensing regulon via the transcriptional regulator PqsR (MvfR) (15, 16). Studies have shown that PqsR also plays a role in many biological activities involving another AQ, namely, 2-heptyl-4-hydroxyquinoline N-oxide (HQNO) (14, 17–19). While the production of both PQS and HQNO involves the transformation of modified anthranilate precursors by PqsABC, their synthesis pathways are known to diverge in one or more ways, since PQS and HQNO require the activities of PqsH and PqsL, respectively (14, 19).

Recent studies have indicated that PQS production also depends on the IQS signal (9). While phosphate limitation induces PQS production (20), initiation of the stringent response by starvation leads to the repression of AQ production (21). Thus, while some "insulated" actions of PQS regulation are clear (22), there is still much to learn about the factors and circumstances that determine how P. aeruginosa activates the PQS pathway in response to environmental challenges (23).

Under conditions that promote the collective movement described as swarming, PQS has been shown to promote a protective response to some antibiotic classes (but not all) (23, 24) and also to protect against phage infection (24). These findings are also related to earlier work reporting that PQS generally limits swarming expansion (18). Additionally, previous studies from our laboratory (12, 25) have produced strong evidence that P. aeruginosa secretes a characteristic sequence of AQs in the first 96 h in monocultures grown on surfaces. However, in most growth environments, P. aeruginosa is likely to coexist and compete with other bacterial species. Detailed examinations of some cocultures and mixed cultures of bacteria have suggested that bacterial species can alter their QS system responses under environmentally competitive conditions in order to respond to messages from other bacterial species, altering their behavior accordingly (5, 26, 27).

Our laboratories have established the utility of combined multimodal chemical imaging as a tool for discerning the spatial and temporal distributions of a range of bacterial compounds. In the present work, we apply comprehensive hyperspectral Raman imaging to characterize the spatiotemporal distribution of AQs produced in response to different stresses. Specifically, we examined the behavior of P. aeruginosa under two kinds of environmental challenges: metabolic stress induced by nutrient limitations and the competitive stress induced by coculturing P. aeruginosa with Escherichia coli. The spatiotemporal chemical information we have obtained about secreted AQs enables us to conclude that while nutrient limitation represses all AQ production during surface growth, other environmental challenges do not modulate PQS and HQNO responses equally.

RESULTS AND DISCUSSION

Surface growth in the presence of E. coli elicits earlier production of PQS in P. aeruginosa. While many reports have annotated PQS as a stress response (16, 24, 28), the triggers for AQ production and PQS response are not clear. Here, we analyzed the
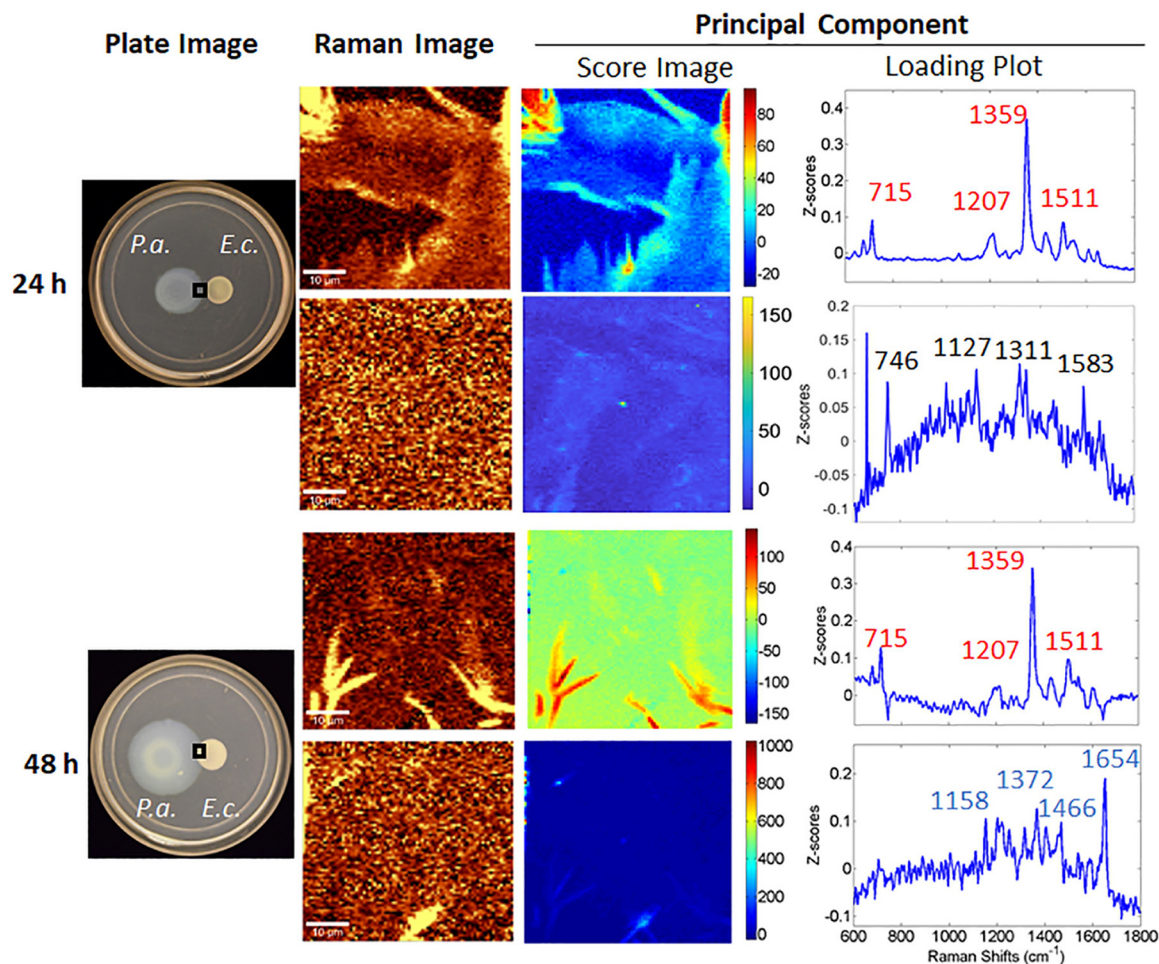
FIG 1 Combined CRM and PCA show that *P. aeruginosa* exhibits signatures of PQS by 48 h when cocultured with *E. coli*. Shown are images of the resultant *P. aeruginosa* and *E. coli* growth on 0.7% agar at 24 h (top) and 48 h (bottom). Raman measurements were taken in the region of the *P. aeruginosa* advancing edge at 24 h and at the intersection of the two strains at 48 h (shown as boxed areas on plates). One representative Raman image and one representative score image are shown for integrations over the 1,330-to-1,380-cm^{-1} (top row) and 1,630-to-1,680-cm^{-1} (bottom row) spectral windows at both 24 h and 48 h. Spectra were acquired and inspected over at least five locations within the region to validate overall consistency. Loading plots and score images of principal components were generated from principal-component analysis of the CRM microspectra acquired over the same region. HQNO and PQS features are labeled in red and blue, respectively. In the 48-h sample, PCA revealed two principal components with distinct features, which represent PQS and HQNO, respectively. Bars, 10 μm.

spatiotemporal aspects of two AQs: 2-heptyl-3-hydroxy-4(1*H*) (PQS) and 2-heptyl-4-hydroxyquinoline *N*-oxide (HQNO). We examined the PQS and HQNO responses of *P. aeruginosa* growing in proximity to *E. coli* K-12, a model lab bacterium that we used as a nonspecific competitor of *P. aeruginosa*. These species were cultured simultaneously by inoculation at a distance of 12 mm from each other on a semisolid agar medium (see Fig. S1 in the supplemental material). At time points (*t*) of 24 h, 48 h, and 96 h, the area between the inoculated spots was imaged using confocal Raman microscopy (CRM), and the results were analyzed using principal-component analysis (PCA) in order to assess the spatiotemporal development of the distribution of signaling molecules in the region between the *P. aeruginosa* and *E. coli* cultures.

Previous studies have demonstrated that *P. aeruginosa* communities growing on semisolid surfaces tend to produce more PQS and HQNO than planktonic cultures (29). When *P. aeruginosa* encounters *E. coli*, we find that PQS appears sooner than when no *E. coli* is present. At 24 h, as the Raman microscopy and PCA results in Fig. 1 confirm, HQNO, with features at 715, 1,207, 1,359, and 1,511 cm^{-1}, is present, but not PQS, in agreement with observations from a *P. aeruginosa* monoculture (shown in Fig. S2). We

also observed a loading plot indicating the presence of *P. aeruginosa* cells with features at 746, 1,127, 1,313, and 1,583 cm^{-1}. However, between 24 and 48 h, *P. aeruginosa* steadily expanded toward *E. coli*, and by 48 h, PQS features (1,158, 1,372, and 1,466 cm^{-1}) appeared, much earlier than the 96-h appearance in monoculture (Fig. S2).

Multipoint inoculation of *P. aeruginosa* shows the same temporal PQS response as that in a single monoculture. Since interaction with *E. coli* was shown to elicit earlier PQS production, we investigated if PQS production is stimulated by any possible competitor. We rationalized that the least competitive coculture conditions would be observed in assays of *P. aeruginosa* with itself. We again used a combination of CRM and PCA tools to examine the intersection area between intersecting colonies of the same *P. aeruginosa* strain. These *P. aeruginosa* self-cocultures exhibited identical surface growth phenotypes, although they were inoculated as two separate points, as shown in the plate assay images (Fig. S3, plate panel). At 48 h, Raman images and PCA confirmed the presence of HQNO in the region where two separate, expanding *P. aeruginosa* colonies meet (Fig. S3c), with features at positions identical to those in a single monoculture inoculation (Fig. S2). At 96 h, in addition to HQNO, PQS features were observed at 1,158, 1,372, and 1,466 cm^{-1}, in agreement with the results of the single-inoculum monoculture experiment. Thus, the results of double inoculation of *P. aeruginosa* (Fig. S3) matched the *P. aeruginosa* monoculture data shown in Fig. S2, in that spectral signatures of PQS were not observed until 96 h. We contrast these monoculture results with the *P. aeruginosa*–*E. coli* coculture results of Fig. 1, in which PQS appears by 48 h. We note that the early appearance of PQS clearly correlates with the presence of *E. coli*, suggesting that this phenomenon is a result of intensified stress from the competition of interspecies coculturing, which is not apparent if *P. aeruginosa* is cocultured with itself.

PQS production is spatially and temporally distinct from HQNO production in the presence of *E. coli*. The results presented above suggest a role for PQS in mediating interactions with a foreign bacterial species. Therefore, we sought information about the detailed spatial distribution of PQS produced in cocultures. CRM imaging was performed at five sequential positions spanning a line along the *P. aeruginosa*–*E. coli* coculture plate, as shown in Fig. 2a.

At 24 h, only HQNO is detected (Fig. 2b). Unsurprisingly, HQNO signatures are apparent in areas 1 to 3, from the distal edge of the *P. aeruginosa* colony to its advancing edge. The optical image (Fig. 2a, top) shows that at 24 h, the cells of *P. aeruginosa* and *E. coli* are not yet in contact. However, HQNO is clearly observed in area 4, the proximal edge of *E. coli* facing *P. aeruginosa*, indicating that HQNO is able to translocate into the *E. coli* colony ahead of the advancing *P. aeruginosa* cells and is able to occupy the area of the *E. coli* community as an exogenous molecule. In Fig. 2b, for area 5, located at the edge of the *E. coli* colony distal from the *P. aeruginosa* cells, the dominant features detected by PCA of CRM microspectra are those of *E. coli* cells. The features apparent at 1,005, 1,333, 1,457, and 1,659 cm^{-1} are in excellent agreement with the Raman spectrum acquired from an *E. coli* monoculture acquired separately (Fig. S4a). The lack of AQ features evidenced by the Raman image over 1,330 to 1,380 cm^{-1} in area 5 (Fig. S5) instead allows *E. coli* cellular chemical features to dominate the PCA output. Moreover, CRM and PCA results from separate *E. coli* and *P. aeruginosa* monoculture samples (shown in Fig. S4a and S4b, respectively) clearly indicate that *E. coli* monoculture shows a cellular fingerprint distinct from that of *P. aeruginosa* and specifically shows no evidence of HQNO-related signals (cf. Fig. S2a and S4a).

Interestingly, the chemical profiles of these five areas shift by the 48-h time point. As the plate image (Fig. 2a, 48 h) shows, *P. aeruginosa* has expanded to contact the *E. coli* colony by this stage. Features of PQS (at 1,159, 1,372, and 1,466 cm^{-1}) are readily apparent, in addition to features of HQNO, within areas 2 and 3, i.e., at the center of *P. aeruginosa* inoculation and at the active intersection between the two strains. Comparison of the loading plots from areas 2 and 3 indicates that PQS is most concentrated in area 3, suggesting that the stress response of *P. aeruginosa* to the proximity of *E. coli*
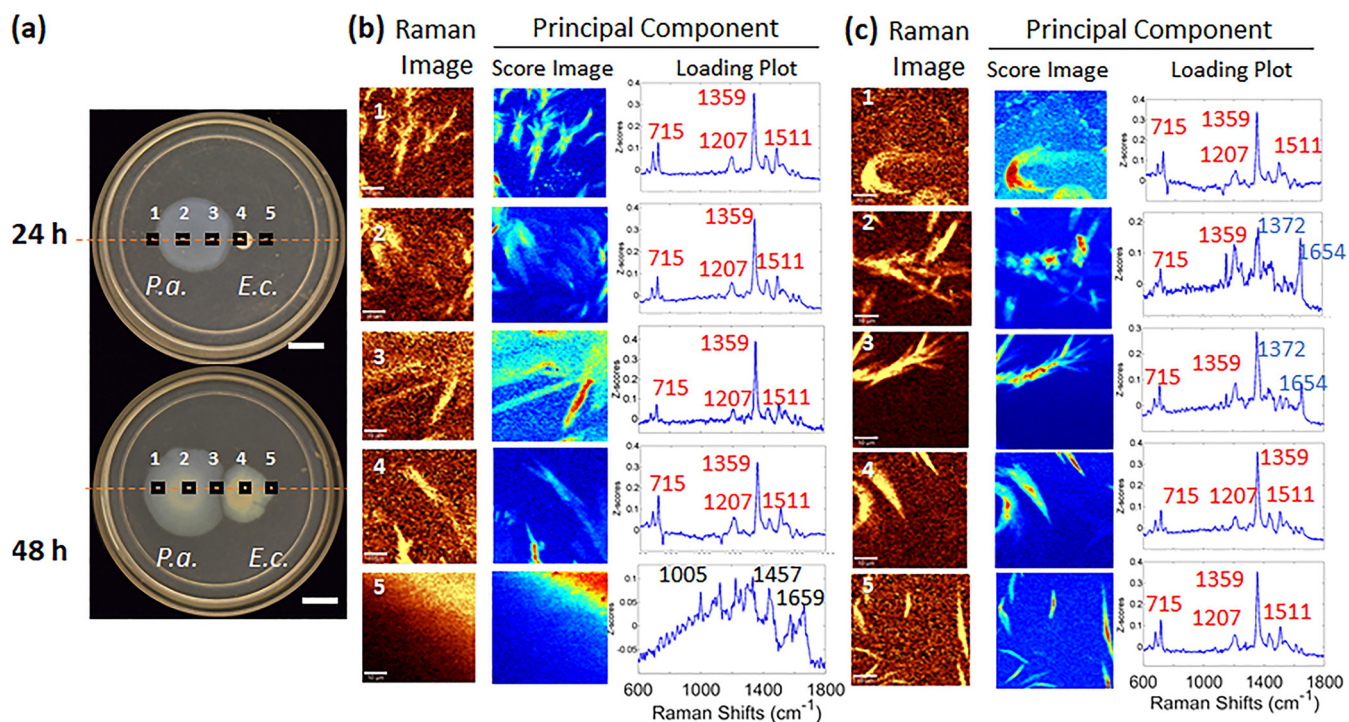
FIG 2 *P. aeruginosa* exhibits PQS signatures only in close proximity to *E. coli*, while HQNO signatures extend beyond the region of *P. aeruginosa* growth. (a) Images of *P. aeruginosa*–*E. coli* coculture plates at 24 h and 48 h (bars, 10 mm). Black squares indicate imaged areas 1 to 5 (along the dashed red lines). At least three regions of interest within each area were picked for scanning. (b) Raman images (integrated over 1,330 to 1,380 cm⁻¹), Z-score spatial maps, and loading plots for the most significant principal component for 24 h as a function of position. Confocal Raman images were integrated over 1,330 to 1,380 cm⁻¹ for areas 1 to 4 and over 2,800 to 3,000 cm⁻¹ for area 5. Principal-component analysis was performed for all areas to generate score images and loading plots. All loading plots showed regions of Raman shifts from 600 to 1,800 cm⁻¹. (c) CRM and PCA results of a 48-h coculture from area 1 to area 5 (all integrated over 1,330 to 1,380 cm⁻¹), showing the locations of features from HQNO (red lettering) and PQS (blue lettering). PQS was detected within areas 2 and 3 at 48 h. Score image values range from low (dark blue) to high (red) in each plot, although the total range differs from plot to plot. All samples were grown on FAB-glucose (12 mM) medium with 0.7% agar (bars, 10 μm).

is highly localized. Another change from the 24-h profile is that HQNO is now apparent in area 5 at 48 h (Fig. 2c). Thus, by 48 h, HQNO has spread far from areas of *P. aeruginosa* growth, to all areas where *E. coli* cells are located. We note how the distributions of HQNO and PQS were markedly different, in that PQS was not detected at these areas away from the point of *P. aeruginosa*–*E. coli* convergence (even at the distal edge of the *P. aeruginosa* colony). These spatial analysis experiments not only demonstrate that PQS is produced later than HQNO in these coculture assays; they also suggest that PQS is first produced preferentially at the intersection of the cocultured strains, where the competitive stress is highest, and at the *P. aeruginosa* colony center, where cells have accumulated to the highest density. These observations clearly indicate that *P. aeruginosa* has the ability to spatially regulate its PQS response (but not HQNO) within just a subset of the community in response to spatially local stimuli.

Metabolic stress boosts PQS production and alters the PQS production pathway. We further probed AQ responses as a function of nutrient availability. We hypothesized that the faster PQS response resulting from *E. coli* interaction shown above (Fig. 1 and 2) could be further intensified if nutrient availability were more limited, because competitive pressures would be more severe. For simplicity, we modified only the carbon source and performed assays with reduced glucose concentrations. While the initial experiments utilized a glucose concentration of 12 mM, here, glucose concentrations were limited to 6 mM or 3 mM, again using CRM in combination with PCA to assess the spatiotemporal attributes of AQ expression at 24 h and 48 h.

As described above, *P. aeruginosa* growing on plates containing 12 mM glucose in a single-species monoculture or self-coculture exhibits PQS at 96 h (Fig. S2 and S3), and
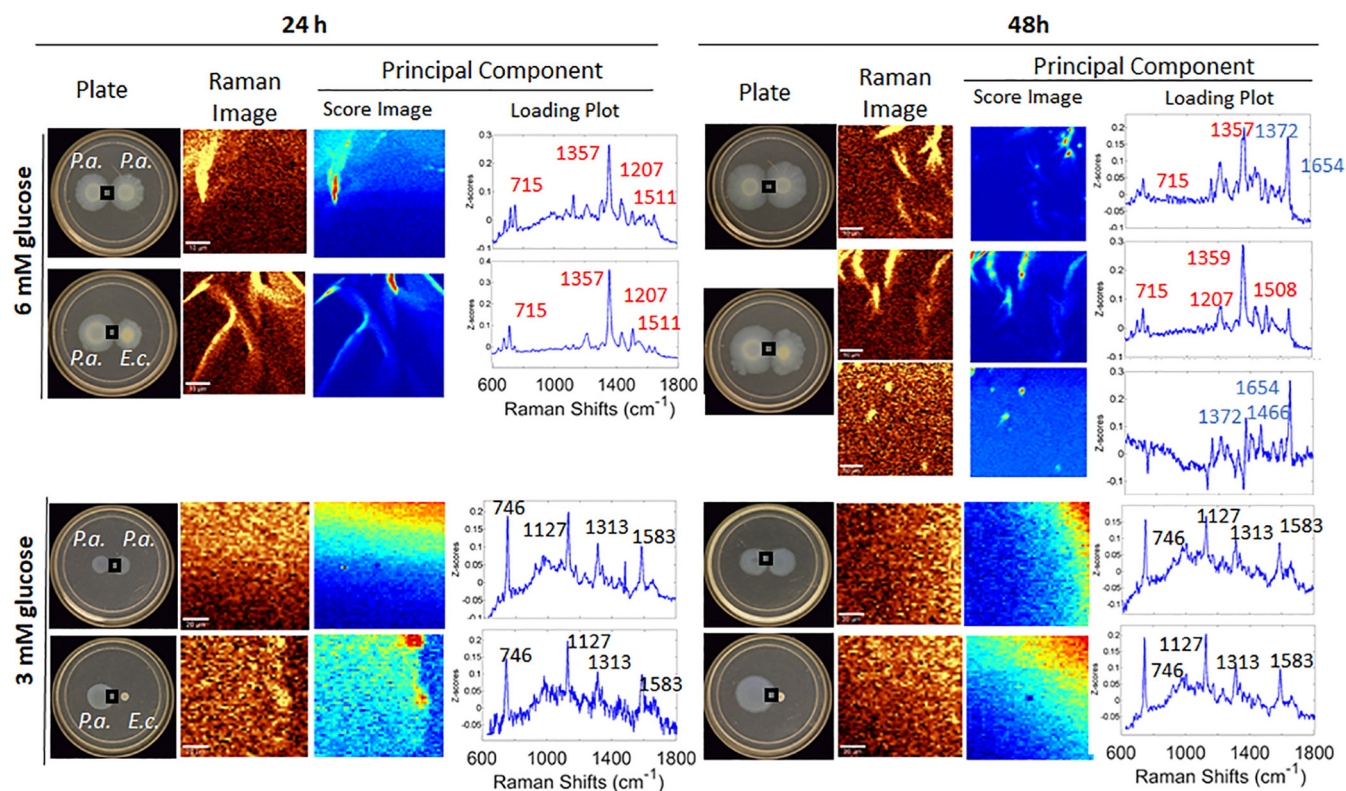
FIG 3 Effects of metabolic stress on PQS production with and without interspecies competition. Imaged areas are boxed on the plates, and at least three regions of interest within each area were picked for scanning. The matrices of CRM and PCA results were acquired as a function of glucose concentration (3 mM and 6 mM) and time (24 h and 48 h) for both *P. aeruginosa* with *P. aeruginosa* and *P. aeruginosa* with *E. coli*. Each panel shows (from left to right) an optical image of the plate, the Raman image, the Z-score image, and the loading plot. For 6 mM glucose samples, Raman images were integrated over the spectral window of 1,330 to 1,380 cm^{-1}, except for the 48-h coculture of *P. aeruginosa* with *E. coli*, which also includes intensities integrated from 1,630 to 1,680 cm^{-1}. For 3 mM glucose samples, Raman images were integrated over the range of 2,800 to 3,000 cm^{-1}. For the 48-h sample in 6 mM glucose only, the first two principal-component Z-score images and loading plots are shown. Score image values range from low (dark blue) to high (red) in each plot, although the total range differs from plot to plot. All samples were grown on FAB-glucose (at 6 mM [top] or 3 mM [bottom]). Bars, 10 μm.

this timing was accelerated to 48 h in *E. coli* competition assays (Fig. 1 and 2). Experiments with reduced levels of glucose show that these PQS responses are conditionally affected by nutrient availability. Figure 3 illustrates a matrix of CRM and PCA results acquired as a function of glucose concentration (3 mM and 6 mM), incubation pairing (*P. aeruginosa*–*P. aeruginosa* and *P. aeruginosa*–*E. coli*), and time (24 h and 48 h). Under the most extreme metabolic stress conditions, i.e., 3 mM glucose, no features characteristic of HQNO or PQS production were observed. We draw this conclusion by examining spectral windows of both 1,330 to 1,380 cm^{-1} (quinolone ring stretching region; Fig. 3) and 2,800 to 3,000 cm^{-1} (C-H stretching region; Fig. S6) based on our prior work (12, 25). The only features detected were those of *P. aeruginosa* cells at 746, 1,127, 1,313, and 1,583 cm^{-1}, independently of time and incubation pairing. Given the adequacy of 3 mM glucose for supporting bacterial growth, which was apparent by visual inspection (Fig. 3, plate panels), we were surprised by the stark contrast in AQ production for these assays. While PQS production is already known to be cell density dependent, it was surprising that colonies of the size observed exhibited no AQ signature even after 96 h (not shown). In combination, the smaller relative expansion and the lack of an AQ signature at 3 mM glucose are clearly consistent with nutrient limitation. This result is in agreement with the findings of prior investigations of the stringent response, where the absence of (p)ppGpp, which accumulates under starvation conditions, was required for production of PQS (21, 30). This reinforces prior genetics work showing that production of any AQ, not just PQS, would require a threshold metabolic state in addition to a quorum population density (21). In compar-
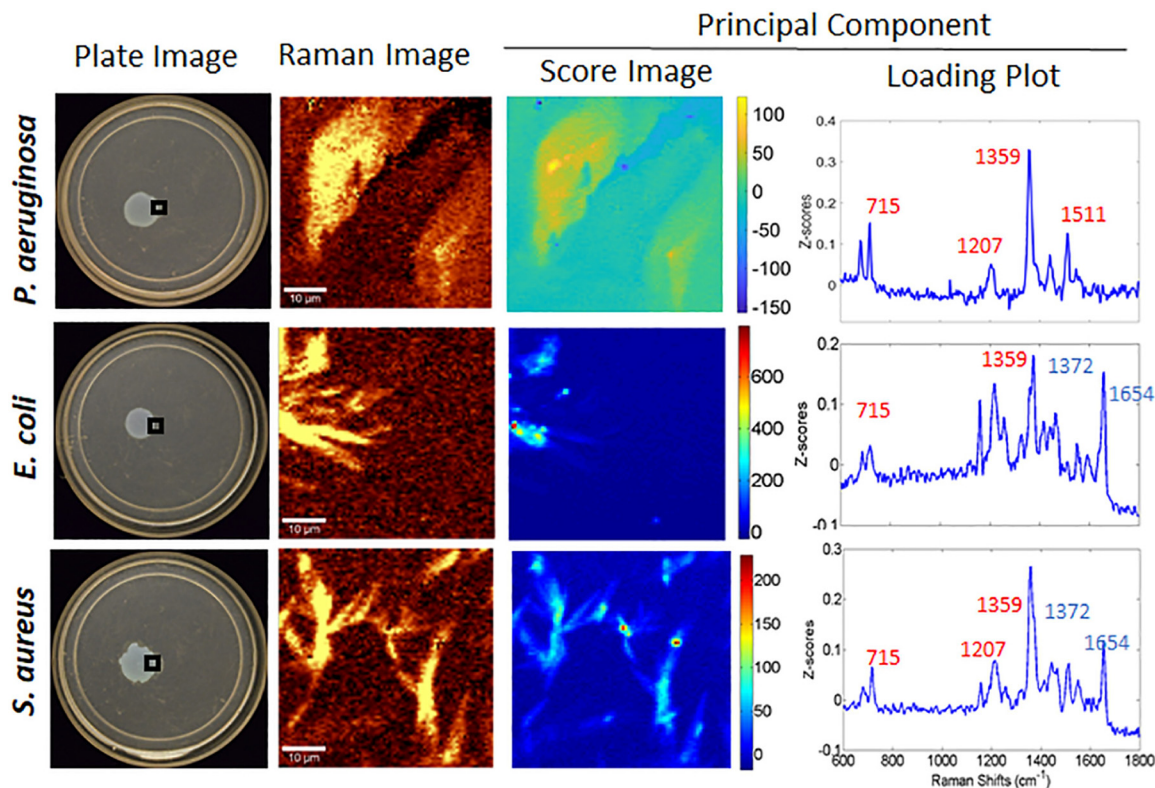
FIG 4 Optical images, Raman images (1,330 to 1,380 cm^{-1}), and PCA of the advancing edge (boxed areas on plates) of *P. aeruginosa* exposed to 1 μl of a *P. aeruginosa*, *E. coli*, or *S. aureus* supernatant. Supernatants were spotted directly on the edge at 18 h postinoculation, and the plate was then returned to the incubator for another 6 h before being removed for testing. All samples were grown on FAB-glucose (12 mM) medium with 0.5% agar. Bars, 10 μm.

ison to setups such as biofilm flow cell assays, where extremely low nutrient concentrations are sufficient to promote QS responses, our results suggest that certain surface growth conditions may require a higher nutrient threshold to elicit an equivalent QS response. Thus, we conclude that the starvation "threshold" required to enable AQ production is a relative target that varies greatly depending on the specific growth conditions.

In assays with 6 mM glucose, PQS is produced in both noncompetitive and competitive modes, i.e., in both *P. aeruginosa*–*P. aeruginosa* cocultures and *P. aeruginosa*–*E. coli* cocultures, as early as 48 h (Fig. 3). While only HQNO is observed in either coculture at 24 h, PQS is observed under both coculture conditions at 48 h. These 6 mM glucose assays represent the only condition we tested under which *P. aeruginosa* alone exhibited a PQS response by 48 h. The collective different HQNO and PQS responses indicate that while competition and nutrient stress can both cue the PQS response, a threshold metabolic state is required for its initiation. This result was apparent for the entire colony with no spatial variation. These results also point to the utility of motility plate assays for conducting these experiments: while ample bacterial growth was exhibited in all assays examined (Fig. 1 to 4; also Fig. S2 to S4), a range of condition-specific AQ responses was observed, mediated by the different scenarios we tested.

Interspecies supernatants induce PQS production in *P. aeruginosa*. Having observed PQS production at the intersection of *P. aeruginosa* and *E. coli* growth, we asked whether this secretion process needed direct interspecies contact between *P. aeruginosa* and *E. coli* or whether a soluble factor could stimulate PQS production. We tested this by adding supernatants from 2-day *E. coli* planktonic cultures to *P. aeruginosa* growing under the same surface conditions used above with ample nutrient levels

(12 mM glucose). Above, we noted production of PQS in response to the presence of *E. coli* within 48 h of coinoculation (Fig. 1). We hypothesized that stimulation of *P. aeruginosa* using a supernatant from an already-grown high-cell-density *E. coli* culture would stimulate PQS production earlier. To test this, an *E. coli*-derived supernatant was added to the growing edge of an 18-h *P. aeruginosa* monoculture plate, and the plate was incubated for another 6 h, thereby achieving a total of 24 h of *P. aeruginosa* growth time. Figure 4 shows clear spectral evidence of the presence of both HQNO and PQS at the advancing edge of *P. aeruginosa*, where the supernatant was pipetted, indicating that soluble factors produced by *E. coli* contained in the small volume (1 μl) of supernatant are sufficient to induce PQS production. Thus, direct contact between *P. aeruginosa* and *E. coli* cells is not necessary to induce *P. aeruginosa* PQS production. We also conclude that 6 h is sufficient to elicit a PQS response under our surface growth conditions. Subsequently, we expanded our investigation to learn if supernatants from bacteria other than *E. coli* would elicit a PQS response. We chose *Staphylococcus aureus* USA300 as a second test strain, because it coexists and competes with *P. aeruginosa* in many clinical settings (27), and it is also important to understand how the behaviors of the two strains are affected by each other. *S. aureus* supernatant was added to the *P. aeruginosa* plates in the same fashion as the *E. coli* samples (Fig. 4). In response to the *S. aureus*-derived supernatant, the level of PQS spiked in these samples in a manner equivalent to that observed with the addition of *E. coli* supernatant. To control for the possible stimulation of PQS by the addition of new nutrients, we tested the responses of *P. aeruginosa* to its own spent medium (Fig. 4, top) and to the growth medium alone as an uninoculated planktonic control (Fig. S7). As shown in both figures, spotting 1 μl of the *P. aeruginosa* supernatant or growth medium was not sufficient to stimulate PQS production. Thus, both *E. coli* and *S. aureus* supernatants elicited PQS production in *P. aeruginosa* during surface colonization, and we conclude that the stress imposed by other bacterial species on *P. aeruginosa* is readily conveyed in soluble factors produced by either species. These results for the addition of supernatants align with the findings of Horspool and Schertzer (31) showing stimulation of the production of *P. aeruginosa* outer membrane vesicles (OMVs) by *E. coli* supernatants. OMVs have been shown by the Schertzer group and others to be a primary delivery mechanism for PQS.

Two-factor interaction model. These experiments clearly illustrate that PQS production is cued by multiple factors. Moreover, we find that PQS production is cued differently, both temporally and spatially, from HQNO production. Our group and others have previously established that surface growth greatly stimulates both HQNO and PQS production (13, 23). However, under surface motile conditions, the appearance of HQNO predictably precedes the appearance of PQS, but HQNO is not modulated equivalently to PQS (12, 32). Here, we present evidence that at least two separate factors promote PQS production during surface growth, and we present a working model to describe the onset of PQS activation (Fig. 5). PQS production, which reflects a regulatory response to the presence of an environmental challenge, is plotted as a function of growth time either without (Fig. 5, top) or with (Fig. 5, bottom) the presence of a competitor (e.g., *E. coli*). PQS levels are represented by three curves, corresponding to the different glucose concentrations used in the present experiments (black for 3 mM, gray for 6 mM, and red for 12 mM). In the absence of *E. coli* (Fig. 5, top), the production of PQS reaches an effective level (indicated by the dashed horizontal line on the plot) in less time when *P. aeruginosa* experiences some metabolic stress in the form of nutrient limitation (6 mM glucose) than when nutrient levels are adequate (12 mM glucose). However, when the organism is grown with more-severe nutrient limitation (3 mM glucose or less), production of PQS, and of all AQs, is repressed. In the presence of competition stress (e.g., *E. coli* or soluble factors from a supernatant of *E. coli* or *S. aureus*) (Fig. 5, bottom), PQS is produced earlier under both 6 mM and 12 mM nutrient conditions. The production of HQNO was essentially binary: when *P. aeruginosa* was growing on surfaces with sufficient nutrients to overcome stringent-response repression, HQNO was produced and detected communitywide. Alternatively, in planktonic
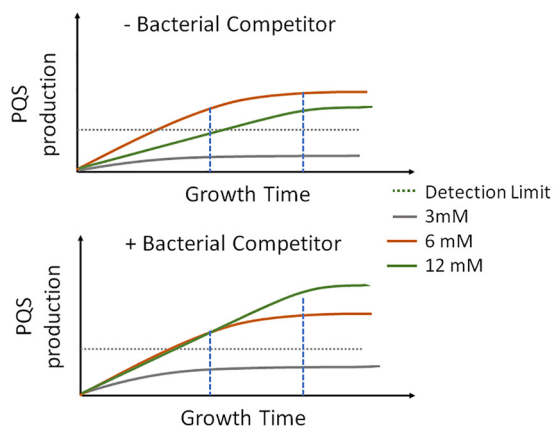
FIG 5 Schematic illustration of the two-factor interaction model. Shown are plots of PQS production as a function of growth time without (top) and with (bottom) a bacterial competitor (e.g., *E. coli*) at 6 mM or 12 mM glucose. The metabolically stressed condition (3 mM glucose) never achieves PQS production. Dashed horizontal lines indicate an effective level of PQS production.

culture and/or under starvation conditions, HQNO was absent. While this simple model does not likely capture the overall regulatory response to all possible environmental stressors, it does highlight the manner in which the two principal environmental challenges studied here interact to affect PQS production. Clearly, further research is needed to determine the differential regulation of PQS and HQNO, as well as the spatial scales on which these AQs are produced and disseminated.

MATERIALS AND METHODS

Bacterial strains. Three bacterial strains were used in these experiments: *Pseudomonas aeruginosa* PAO1C (33), *Escherichia coli* K-12 (34), and *Staphylococcus aureus* (methicillin-resistant *S. aureus* [MRSA]) USA300 (35).

Culturing and surface assay conditions. All bacterial strains were grown planktonically overnight to an optical density at 600 nm (OD$_{600}$) of ≈1.0 in FAB–glucose at 37°C with shaking at 240 rpm. Plates were made by adding 10 ml of sterile FAB-glucose (12 mM, 6 mM, or 3 mM glucose) solidified with 0.5% (wt/vol) Noble agar (or 0.7% [wt/vol] agar, as noted, for select experiments) to 60-mm petri dishes, a procedure similar to our previously reported method (13, 36). For monoculture plates, *P. aeruginosa* was spot-inoculated by pipetting 1 μl of a planktonic culture onto the center of the plate. For cocultured plates, 1 μl of each planktonic culture was simultaneously spot-inoculated at a distance of 12 mm, centered in the middle of the plate, as shown in Fig. S1. For experiments in which a supernatant was added, the supernatant was generated from 2-day planktonic cultures (*E. coli* was cultured in FAB-glucose, and *S. aureus* was cultured in LB) and isolated by centrifugation at 14,000 rpm for 2 min, followed by filtration through a 0.2-μm-pore-size filter. A 1-μl volume of supernatant was then added to those assay plates by pipetting it onto the advancing edge of the *P. aeruginosa* area. After inoculation, all assay plates were covered and left undisturbed until the cells were completely absorbed into the agar. Plates were then inverted and incubated at 30°C in a humidity-controlled (85% relative humidity [RH]) incubator until the desired time. Optical images of plate assay results were acquired using a Nikon D3300 camera (Nikon, Melville, NY) with an 18- to 55-mm f/3.5-5.6G VR II zoom lens.

Raman imaging and PCA. Raman microspectra of the standards (PQS and HQNO) were taken by averaging 10 spectra with an integration time of 0.5 s each. CRM imaging was performed as described previously (13). Briefly, Raman images were acquired by scanning over a selected area of interest on the plate, acquiring a full Raman spectrum at each image pixel using a 40× air objective (numerical aperture [NA], 0.6). Multipoint scans were carried out in the same fashion by laterally moving the sample stage to reach the desired position for each spectral acquisition. Images consisted of 80 × 80 pixels obtained at an integration time of 100 ms per spectrum. Spectra were acquired and averaged over at least five regions of interest within each numbered area. MATLAB was used to perform principal-component analysis (PCA) using previously described custom scripts (37) to extract chemical information from the data set. In addition to PCA, we reconstructed Raman images integrated over spectral window from 1,330 to 1,380 cm^{-1}, indicative of differences in quinolone ring stretching for AQs, and 2,800 to 3,000 cm^{-1}, indicative of C-H bond stretching for all biochemical cellular components (11, 25). Figure S2 illustrates CRM data acquisition and analysis as applied to a *P. aeruginosa* PAO1C monoculture. Because the coexpression of HQNO and PQS can produce PCA features with a complex line shape, these features were fit to a sum of two Voigt profiles, as shown in Fig. S8, to assess the presence of both components.

SUPPLEMENTAL MATERIAL

Supplemental material is available online only.

FIG S1, TIF file, 0.5 MB.
FIG S2, TIF file, 0.9 MB.
FIG S3, TIF file, 1.1 MB.
FIG S4, TIF file, 0.6 MB.
FIG S5, TIF file, 0.4 MB.
FIG S6, TIF file, 0.8 MB.
FIG S7, TIF file, 0.5 MB.
FIG S8, TIF file, 0.2 MB.

ACKNOWLEDGMENTS

REFERENCES

1. Costerton JW, Stewart PS, Greenberg EP. 1999. Bacterial biofilms: a common cause of persistent infections. Science 284:1318–1322. https://doi.org/10.1126/science.284.5418.1318.
2. Hall-Stoodley L, Costerton JW, Stoodley P. 2004. Bacterial biofilms: from the natural environment to infectious diseases. Nat Rev Microbiol 2:95–108. https://doi.org/10.1038/nrmicro821.
3. Latifi A, Winson MK, Foglino M, Bycroft BW, Stewart G, Lazdunski A, Williams P. 1995. Multiple homologs of LuxR and LuxI control expression of virulence determinants and secondary metabolites through quorum sensing in Pseudomonas aeruginosa PAO1. Mol Microbiol 17:333–343. https://doi.org/10.1111/j.1365-2958.1995.mmi_17020333.x.
4. Passador L, Cook JM, Gambello MJ, Rust L, Iglewski BH. 1993. Expression of Pseudomonas aeruginosa virulence genes requires cell-to-cell communication. Science 260:1127–1130. https://doi.org/10.1126/science.8493556.
5. Atkinson S, Williams P. 2009. Quorum sensing and social networking in the microbial world. J R Soc Interface 6:959–978. https://doi.org/10.1098/rsif.2009.0203.
6. Daniels R, Vanderleyden J, Michiels J. 2004. Quorum sensing and swarming migration in bacteria. FEMS Microbiol Rev 28:261–289. https://doi.org/10.1016/j.femsre.2003.09.004.
7. Miller MB, Bassler BL. 2001. Quorum sensing in bacteria. Annu Rev Microbiol 55:165–199. https://doi.org/10.1146/annurev.micro.55.1.165.
8. Parsek MR, Greenberg EP. 2000. Acyl-homoserine lactone quorum sensing in Gram-negative bacteria: a signaling mechanism involved in associations with higher organisms. Proc Natl Acad Sci U S A 97:8789–8793. https://doi.org/10.1073/pnas.97.16.8789.
9. Lee J, Zhang LH. 2015. The hierarchy quorum sensing network in Pseudomonas aeruginosa. Protein Cell 6:26–41. https://doi.org/10.1007/s13238-014-0100-x.
10. Camilli A, Bassler BL. 2006. Bacterial small-molecule signaling pathways. Science 311:1113–1116. https://doi.org/10.1126/science.1121357.
11. Ha DG, Merritt JH, Hampton TH, Hodgkinson JT, Janecek M, Spring DR, Welch M, O'Toole GA. 2011. 2-Heptyl-4-quinolone, a precursor of the Pseudomonas quinolone signal molecule, modulates swarming motility in Pseudomonas aeruginosa. J Bacteriol 193:6770–6780. https://doi.org/10.1128/JB.05929-11.
12. Baig N, Polisetti S, Morales-Soto N, Dunham SJB, Sweedler JV, Shrout JD, Bohn PW. 2016. Label-free molecular imaging of bacterial communities of the opportunistic pathogen Pseudomonas aeruginosa. Proc SPIE Int Soc Opt Eng 9930:993004. https://doi.org/10.1117/12.2236695.
13. Baig NF, Dunham SJB, Morales-Soto N, Shrout JD, Sweedler JV, Bohn PW. 2015. Multimodal chemical imaging of molecular messengers in emerging Pseudomonas aeruginosa bacterial communities. Analyst 140:6544–6552. https://doi.org/10.1039/c5an01149c.
14. Dulcey CE, Dekimpe V, Fauvelle DA, Milot S, Groleau MC, Doucet N, Rahme LG, Lepine F, Deziel E. 2013. The end of an old hypothesis: the Pseudomonas signaling molecules 4-hydroxy-2-alkylquinolines derive

from fatty acids, not 3-ketofatty acids. Chem Biol 20:1481–1491. https://doi.org/10.1016/j.chembiol.2013.09.021.
15. Coleman JP, Hudson LL, McKnight SL, Farrow JM, III, Calfee MW, Lindsey CA, Pesci EC. 2008. Pseudomonas aeruginosa PqsA is an anthranilate-coenzyme A ligase. J Bacteriol 190:1247–1255. https://doi.org/10.1128/JB.01140-07.
16. Häussler S, Becker T. 2008. The pseudomonas quinolone signal (PQS) balances life and death in Pseudomonas aeruginosa populations. PLoS Pathog 4:e1000166. https://doi.org/10.1371/journal.ppat.1000166.
17. Maura D, Rahme LG. 2017. Pharmacological inhibition of the Pseudomonas aeruginosa MvfR quorum-sensing system interferes with biofilm formation and potentiates antibiotic-mediated biofilm disruption. Antimicrob Agents Chemother 61:e01362-17. https://doi.org/10.1128/AAC.01362-17.
18. Guo Q, Kong W, Jin S, Chen L, Xu Y, Duan K. 2014. PqsR-dependent and PqsR-independent regulation of motility and biofilm formation by PQS in Pseudomonas aeruginosa PAO1. J Basic Microbiol 54:633–643. https://doi.org/10.1002/jobm.201300091.
19. Drees SL, Ernst S, Belviso BD, Jagmann N, Hennecke U, Fetzner S. 2018. PqsL uses reduced flavin to produce 2-hydroxylaminobenzoylacetate, a preferred PqsBC substrate in alkyl quinolone biosynthesis in Pseudomonas aeruginosa. J Biol Chem 293:9345–9357. https://doi.org/10.1074/jbc.RA117.000789.
20. Meng X, Ahator SD, Zhang LH. 2020. Molecular mechanisms of phosphate stress activation of Pseudomonas aeruginosa quorum sensing systems. mSphere 5:e00119-20. https://doi.org/10.1128/mSphere.00119-20.
21. Schafhauser J, Lepine F, McKay G, Ahlgren HG, Khakimova M, Nguyen D. 2014. The stringent response modulates 4-hydroxy-2-alkylquinoline biosynthesis and quorum-sensing hierarchy in Pseudomonas aeruginosa. J Bacteriol 196:1641–1650. https://doi.org/10.1128/JB.01086-13.
22. Lin JS, Cheng JL, Wang Y, Shen XH. 2018. The Pseudomonas quinolone signal (PQS): not just for quorum sensing anymore. Front Cell Infect Microbiol 8:230. https://doi.org/10.3389/fcimb.2018.00230.
23. Morales-Soto N, Dunham SJB, Baig NF, Ellis JF, Madukoma CS, Bohn PW, Sweedler JV, Shrout JD. 2018. Spatially dependent alkyl quinolone signaling responses to antibiotics in Pseudomonas aeruginosa swarms. J Biol Chem 293:9544–9552. https://doi.org/10.1074/jbc.RA118.002605.
24. Bru JL, Rawson B, Trinh C, Whiteson K, Hoyland-Kroghsbo NM, Siryaporn A. 2019. PQS produced by the Pseudomonas aeruginosa stress response repels swarms away from bacteriophage and antibiotics. J Bacteriol 201:e00383-19. https://doi.org/10.1128/JB.00383-19.
25. Morales-Soto N, Cao T, Baig NF, Kramer KM, Bohn PW, Shrout JD. 2018. Surface-growing communities of Pseudomonas aeruginosa exhibit distinct alkyl quinolone signatures. Microbiol Insights 11:1178636118817738. https://doi.org/10.1177/1178636118817738.
26. Filkins LM, Graber JA, Olson DG, Dolben EL, Lynd LR, Bhuju S, O'Toole GA. 2015. Coculture of Staphylococcus aureus with Pseudomonas aeruginosa drives S. aureus towards fermentative metabolism and reduced

mSphere®

viability in a cystic fibrosis model. J Bacteriol 197:2252–2264. https://doi
.org/10.1128/JB.00059-15.

27. Woods PW, Haynes ZM, Mina EG, Marques CNH. 2019. Maintenance of *S. aureus* in co-culture with *P. aeruginosa* while growing as biofilms. Front Microbiol 9:3291. https://doi.org/10.3389/fmicb.2018.03291.

28. Lee J, Wu J, Deng Y, Wang J, Wang C, Wang J, Chang C, Dong Y, Williams P, Zhang LH. 2013. A cell-cell communication signal integrates quorum sensing and stress response. Nat Chem Biol 9:339–343. https://doi.org/10.1038/nchembio.1225.

29. Cao TY, Morales-Soto N, Jia J, Baig NF, Dunham SJB, Ellis J, Sweedler JV, Shrout JD, Bohn PW. 2019. Spatiotemporal dynamics of molecular messaging in bacterial co-cultures studied by multimodal chemical imaging. Proc SPIE Int Soc Opt Eng 10863:108630A. https://doi.org/10.1117/12.2501349.

30. Schuster M, Greenberg EP. 2007. Early activation of quorum sensing in *Pseudomonas aeruginosa* reveals the architecture of a complex regulon. BMC Genomics 8:287. https://doi.org/10.1186/1471-2164-8-287.

31. Horspool AM, Schertzer JW. 2018. Reciprocal cross-species induction of outer membrane vesicle biogenesis via secreted factors. Sci Rep 8:9873. https://doi.org/10.1038/s41598-018-28042-4.

32. Abisado RG, Benomar S, Klaus JR, Dandekar AA, Chandler JR. 2018. Bacterial quorum sensing and microbial community interactions. mBio 9:e02331-17. https://doi.org/10.1128/mBio.02331-17.

33. Holloway BW. 1955. Genetic recombination in *Pseudomonas aeruginosa*. J Gen Microbiol 13:572–581. https://doi.org/10.1099/00221287-13-3-572.

34. Lederberg J, Tatum E. 1946. Gene recombination in *Escherichia coli*. Nature 158:558. https://doi.org/10.1038/158558a0.

35. Tenover FC, Goering RV. 2009. Methicillin-resistant *Staphylococcus aureus* strain USA300: origin and epidemiology. J Antimicrob Chemother 64:441–446. https://doi.org/10.1093/jac/dkp241.

36. Shrout JD, Chopp DL, Just CL, Hentzer M, Givskov M, Parsek MR. 2006. The impact of quorum sensing and swarming motility on *Pseudomonas aeruginosa* biofilm formation is nutritionally conditional. Mol Microbiol 62:1264–1277. https://doi.org/10.1111/j.1365-2958.2006.05421.x.

37. Ahlf DR, Masyuko RN, Hummon AB, Bohn PW. 2014. Correlated mass spectrometry imaging and confocal Raman microscopy for studies of three-dimensional cell culture sections. Analyst 139:4578–4585. https://doi.org/10.1039/c4an00826j.